Microstructure, Mechanical and Thermal Properties of Plasma-Sprayed W/SiC Metal Matrix Composite Coating†

FAHIM F. Narges* and KOBAYASHI Akira**

Abstract

A functionally graded SiC/W metal matrix composite (MMC) has been successfully produced by gas tunnel type plasma spraying. The starting powder was a mixture of 12% W and 88 wt% SiC. The effect of plasma gun current on the microstructure, mechanical and thermal conductivity properties was investigated. The results revealed that the reaction phases, namely tungsten silicides (WSi_2, W_5Si_3) and tungsten carbides (WC, W_2C), were not formed in various processing conditions. The presence of WO_3 was detected in the composite deposits, which indicated that the tungsten partially oxidized during plasma spraying. Also, the composite deposited was dense and nearly free of pores due to the small mismatch between the coefficients of thermal expansion (CTE) for W and SiC. Microhardness values gradually decreased as a function of input current due to the formation of WO_3 and the decomposition of SiC particles in the high temperature flame region. A thermal conductivity as high as ~ 59 W/m.K was obtained. It was found that both tungsten oxide and structure imperfections have a significant influence on the thermal conductivity and mechanical properties.

KEYWORDS: (W/SiC Metal-Matrix Composite), (Gas Tunnel Type Plasma Spraying), (Microstructure), (Microhardness), (Abrasive Wear), (Thermal Diffusivity), (Thermal Conductivity).

1. Introduction

Fusion reactors are considered as a good source of energy for civilization in the future. They are expected to with electrical power of ~ 1500 MW. In the field of fusion reactor technology, one of the most important issues is the development of high performance plasma facing material (PFM). The divertor as a plasma facing component in fusion reactors, which is exposed to high heat flux (HHF) due to the bombardment by energetic particles, requires high thermal conductivity, excellent thermal shock resistance, good control of plasma particles and good connection with heat sink materials for active cooling. High thermal efficiency, resistance against radiation damage, low activation are further important issues.

Tungsten has a body centered cubic structure (bcc), a high melting point (3420 ^{o}C), good erosion resistance to welding and sparking, low vapor pressure (1.3 x 10^{-7} Pa at Tmelt), high strength and dimensional stabilities at elevated temperatures, low thermal expansion coefficient (4.5 x10^{-6} /K), and high thermal conductivity (167 W/m.K). These properties make tungsten a candidate for plasma facing material for the divertor region in International Thermonuclear experimental reactors (ITER). Unfortunately, there are serious drawbacks in using tungsten as a structure material of the divertor such as decrease of the thermal conductivity, and embrittlement (increase of the ductile-to-brittle transition temperature and loss of ductility) [1]. The issue of reduced thermal conductivity was solved by adopting a functionally graded material that exhibits a smooth property transition (i.e. thermal expansion coefficient).

Moreover, SiC exhibits high mechanical and physical properties and has low price. Hence it has been proposed to use tungsten and SiC metal matrix composites as plasma facing materials for fusion reactors. W/ SiC metal matrix composite materials show a high thermal conductivity (TC) and a sufficiently low coefficient of thermal expansion (CTE). One unique advantage of the composites is that their CTE can be tailored by regulating the type and content of particle reinforcement (SiC). Plasma-spraying has been used to produce protective coatings and free standing near-net shapes of a wide range of material, such as, metal alloys, intermetallics, ceramics and composites [2]. Plasma spraying is a technique of rapid melting and solidification of feedstock. However, Gas tunnel type plasma spraying is characterized by stable plasma with higher temperature, which is sufficient to melt refractory material. Gas tunnel plasma spraying has been used to deposit ceramic coating and refractory metals [3-5]. The microstructure in the

† Received on November 10, 2006
* Foreign Visiting Researcher
** Associate Professor

Transactions of JWRI is published by Joining and Welding Research Institute, Osaka University, Ibaraki, Osaka 567-0047, Japan

sprayed materials, which formed under very high temperature (5000-12000 K), high velocity (200-700 m/s) and rapid solidification rate (10^{5-7} K/s), displays some difference from that obtained by other fabrication processes. Consequently, the sprayed composites (W/SiC) would exhibit difference in some properties such as thermal conductivity and mechanical properties. To our knowledge, no data about such properties for plasma-sprayed W/SiC are available. In the present work, W/ SiC metal matrix composite was plasma sprayed, with tungsten powder containing 88 wt% SiC particles, by using gas tunnel plasma spraying. Mechanical and thermal properties were studied as a function of gun current. In addition, the microstructure of the composite and various structural phases were discussed.

2. Experimental

2.1. W/SiC composite preparation

Starting powder materials of W (purity 99.9 %, particle size < 5μm) and SiC (purity 97 %, particle size < 45 μm) were weighed in the proportion 12 W-88 SiC wt. %. Then the powders were mixed manually and dried for 1 h at 100 °C. Powder feedstock was fed to the plasma torch inside the nozzle. The details of the plasma spraying parameters are depicted in **Table 1**. Within the torch, a stream of Ar gas was transformed in the plasma by means of a direct current arc and ejected from nozzle. The W/SiC to be deposited is injected in to the plasma flame where it is melted and accelerated toward a stainless steel substrate AISI 304 with dimension 50 mm (long) x 50 mm (wide) x 3mm (thick). Before spraying deposition, the substrate was grit blasted using alumina powders to clean and roughen the surface to improve the film adhesion. Then, it was cleaned with acetone to remove any grease.

Plasma spraying was carried out by using gas tunnel type plasma spraying (GTPS), which was developed in Osaka University [3]. **Figure 1** shows a schematic diagram of the GTPS system that was used in this study. The system composed of one cathode rod and two anodes; one of them is a hollow anode and the other is a nozzle anode, which form a two stage cascade arc scheme. The discharge system has a special designed space between the two anodes, which is characterized by gas channels on its walls such that the gas can flow into the hallow cavity of the space and formed a gas tunnel in its axial region. Firstly, the plasma is formed in the hollow anode and then emitted like a flame outside the exit of the nozzle, which is well confined in the tunnel due to the thermal pinch effect and can be much higher in temperature and more stable than traditional free-standing arc torches [6]. The first-stage of the system is initiated by a DC power source (PS-A) which can provide current as high as 140 A and power as high as 10 KW and high voltage as high as 3 KV at a frequency of 120 Hz. While the second stage is started by another more powerful DC supply (PS-B) that can provide current as high as 500 A and power of 30 KW to amplify the plasma power. Through the two stages, two gas inlets were used to feed working gas. The working gas for the first stage is fed through the rear inlet around the cathode, while the carrier gas for the second stage is fed from the channels on the space wall. In front of the plasma, a movable substrate holder was fitted to change the distance between the substrates and the nozzle anode exit. In this study, the spraying deposition of W/SiC was performed under various currents of the first stage gun 50-120 A, while the second stage discharge vortex was maintained with a current of 450 A.

Table 1 Spraying parameters for the preparation of W/SiC metal matrix composite coating.

Gun current [A]	50, 80, 100,120,
DC plasma vortex current [A]	450
Primary gas flow rate, Q [Ar, l/min]	150
Carrier gas[Argon, l/min]	10
Powder feed rate, w [g/min]	5
Spraying distance, L [mm]	50
Spraying time, t [sec]	30
Nozzle diameter [mm]	20
Traverse rate [mm/s]	20

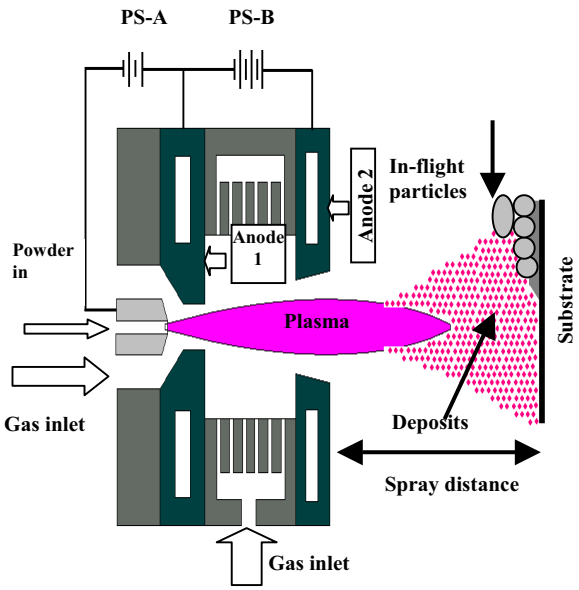

Fig.1 Schematic diagram of the gas tunnel type plasma spraying system.

Table 2 Thermal properties of SiC and Tungsten coating materials used in this study.

Material	CTE* (*RT, 10^{-6}/K*)	Melting Point (^oC)	Thermal Conductivity (*RT, W/K m*)
SiC	4.02	2800	125.6
W	4.5	3420	167

** Coefficient of linear thermal expansion*

2.2. XRD and microstructure characterization

The phases composition of feedstock powder and composite deposits were identified by a JEOL JDX-3530M X-ray diffractometer with Cu K-α radiation (λ = 1.54) at 40 kV and 40 mA with a scanning rate 0.01 ^{o}/s and a scan speed of 1 ^{o}/min in a 2θ range from 20 to 100 ^{o}. A scanning electron microscope (SEM, ERA 8800 FE) with energy dispersive X-ray analysis (EDX) was utilized to characterize the microstructure, morphology and chemical composition of the various phases. Some composite samples were cut and embedded in resin and polished to have their cross-section observed by SEM.

2.3. Mechanical properties

2.3.1. Microhardness estimation

A Vicker's indenter was used to measure the hardness using an Akashi AAV-500 series microhardness tester. The Vicker's microhardness measurements were done on polished and buffed surfaces with load: 200g, load time: 20 s and T= 25 ^{o}C. At least ten indentations were made for each load to provide satisfactory statistics.

2.3.2. Abrasive wear test

The abrasive wear tests were conducted on W/ SiC composite in air without lubricant using a SUGA ABRASION TESTER which follows the NUS-ISO-3 standard. The specimens were fixed on a movable plate and moved horizontally (oscillation mode) a distance of 1cm under load 10 g on a slightly moving wheel (10 mm/min) covered with a strip of SiC paper. The wide of the wheel is 1 cm and the contacted area with the specimen is 1cm^2. The specimens were exposed to move against the abrasive wheel in stroke number interval (5-20). For all specimens the weight loss was measured before and after wear using a 6 digits electronic balance.

2.4. Thermal conductivity measurement

Thermal diffusivity measurements were measured by means of the laser flash technique using the Laser Flash Thermal Constant Analyzer (TC7000, ULVAC) at room temperature. The laser was radiated in pulses; the laser energy was 4 J and width of 0.94 ms. An unfocused laser pulse was absorbed into the surface of a disk-shaped sample of (10 mm diameter) and (2.5-3 mm thick), causing homogeneous heating. This method is based on the principle of measuring the transportation time of the heat pulses that are produced by laser pulses. This transportation time is related to the sample thickness and thermal diffusivity. The mathematical analysis of this temperature/time function allowed the determination of the thermal diffusivity, α. These values were then combined with measurement of the geometric density (ρ) of samples and specific heat (C_p) to arrive at thermal conductivity (k), according to the following equation:

$$k = \rho_s C_p \alpha, \qquad (1)$$

The thermal properties of the starting material were summarized in **Table 2**.

3. Results and Discussion

3.1. XRD and morphology of feedstock powder

Figure 2 shows the morphology and X-ray diffraction pattern of 12 W-88 SiC wt %, of the feedstock powder. It is seen that the tungsten and silicon carbide were not uniformly mixed owning to the density difference between tungsten (ρ = 19.3 g/cm^3) and silicon carbide (ρ = 3.21 g/cm^3). The silicon carbide has an angular morphology. Clearly, the hard tungsten powder particles stuck on silicon carbide powder particles as marked in fig. 2 by circle. The peaks corresponding to α-SiC (100), (101), (103), (200), and (201) planes were clearly presented. Moreover, the (002), (110), (112), and (004) peaks due to the presence of β-SiC have been detected. Obviously, the peaks of planes (110), (200), (211), and (220) were due to pure α-Tungsten. Consequently, the feedstock powder is a mixture of 2H-SiC and α-W, as clear from the XRD pattern.

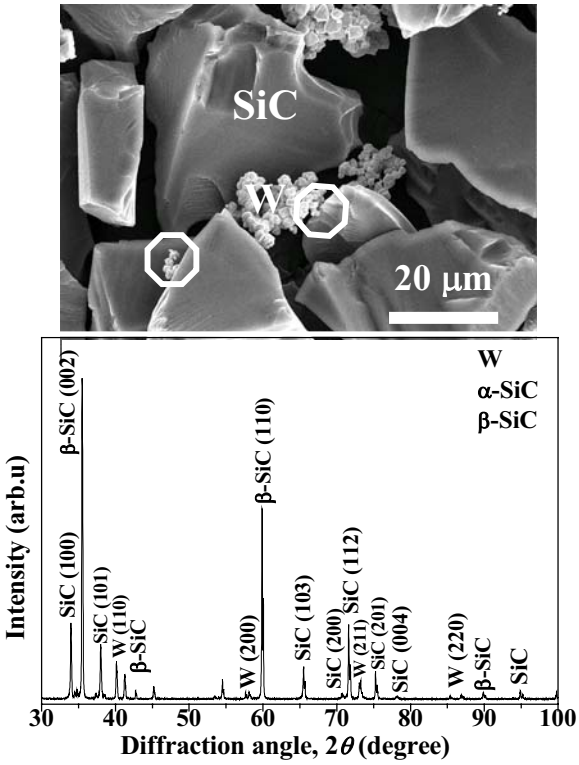

Fig.2 SEM micrograph and XRD diffraction pattern of (88 % SiC + 12 % W) feedstock powder.

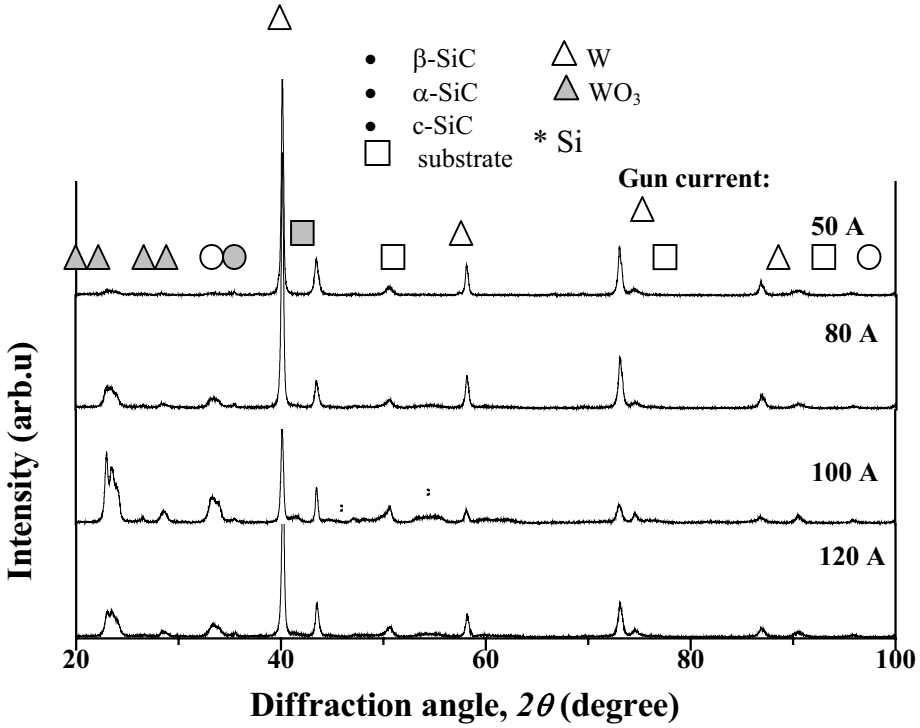

Fig.3 XRD patterns of W/SiC composite as a function of gun current.

3.2. XRD and microstructure observation of W/SiC composite

Figure 3 shows the XRD patterns of the plasma sprayed W/SiC composite deposits. With an increase in the gun current, the intensity of the WO_3 peaks [of planes (002), (020), 021), and (112)] increased, from 50 to 100 A. Hegetüs et al. [7] noted that WO_2 was observed after oxidizing alpha tungsten in moist hydrogen at about 740 ^oC. Their anticipated reaction is expressed as follows:

$$W + 2H_2O = WO_2 + H_2 \quad (2)$$

Bigey et al. [8] observed various oxidation states of tungsten oxides using XPS technology. They concluded that the reduction reaction occurred as follows:

$$WO_3 \Rightarrow WO_{2.9}(at 620^oC) \quad (3)$$

$$WO_3 and WO_{2.9} \Rightarrow WO_2(at 793^oC) \quad (4)$$

$$WO_2 \Rightarrow W(>900^oC) \quad (5)$$

Also the oxidation of tungsten was explained using thermodynamic analysis by Kang and Kang [9]. In our case, it is well known that the plasma spraying used high temperatures (5000-12000 ^oC) and high velocities (200-700 m/s) [10, 11]. Thus, the time required for formation of Tungsten oxides (WO_x) was not enough, due to the rapid solidification rate of liquid/semi-liquid droplets in the range of 10^{5-7}K/s [12]. As a result reactions (2) to (5) could not occur. When droplets impinged on the substrate, the droplets' temperature rapidly decreased to near substrate temperature due to the large temperature gradient between the plasma torch and the substrate, as mentioned by many authors [10, 13-14]. A small number of tungsten particles were oxidized to tungsten oxide vapor (WO_3(g)) in the high temperature plasma jet of ~ 4200 K and became WO_3(S) at the deposits by rapid solidification [9]. It is seen that , the SiC decomposition increased as the gun current increased as evidenced by the presence of silicon peaks of planes (220) and (311) especially at gun current 100 A, as shown in fig. 3. According to Seng and Barnes [15], possible reaction between W and SiC can be expressed as follows:

$$W + SiC \rightarrow WC + Si \quad (6)$$

$$5W + 2SiC \rightarrow 2W_2C + WSi_2 \quad (7)$$

$$W + 2SiC \rightarrow 2C + WSi_2 \quad (8)$$

$$8W + 3SiC \rightarrow W_5Si_3 + 3WC \quad (9)$$

In our case the mixture of W-SiC powder was fed into the plasma jet in the internal powder injection gun by the plasma gas and carrier gas (Ar). The powder particles heated, then melted and solidified at the substrate. In this case, SiC did not undergo the chemical reaction with liquid W to form such compounds of tungsten silicides and tungsten carbides as confirmed by the absence of its peaks in the XRD pattern (Fig.3). There is not enough time for the formation of WSi_2 and W_5Si_3 due to the rapid solidification rate of liquid/semi-liquid droplets in the range of 10^{5-7} K/s. However, tungsten carbides (W_2C and WC) did not form owing to the absence of carbon in the deposit, which reacted with oxygen and escaped as CO_2 and CO according to the following equations:

$$SiC_{(S)} + O_{2(g)} = Si_{(s,l)} + CO_{2(g)} \quad (10)$$

$$SiC_{(S)} + 1/2O_{2(g)} = Si_{(s,l)} + CO_{(g)} \quad (11)$$

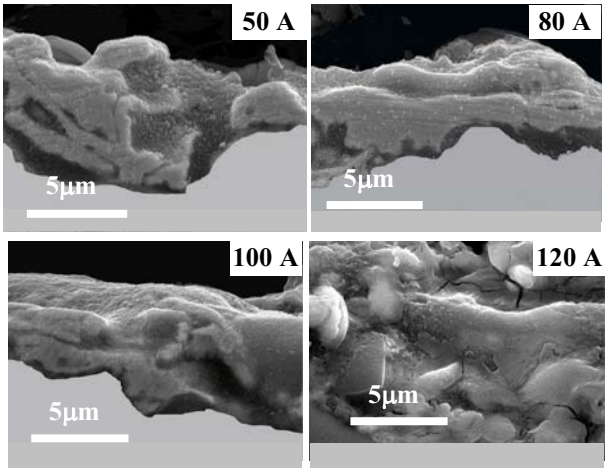

Fig. 4 SEM micrographs of cross-section of W / SiC composite prepared by gas tunnel plasma spraying at various gun current of 50, 80,100 and 120A.

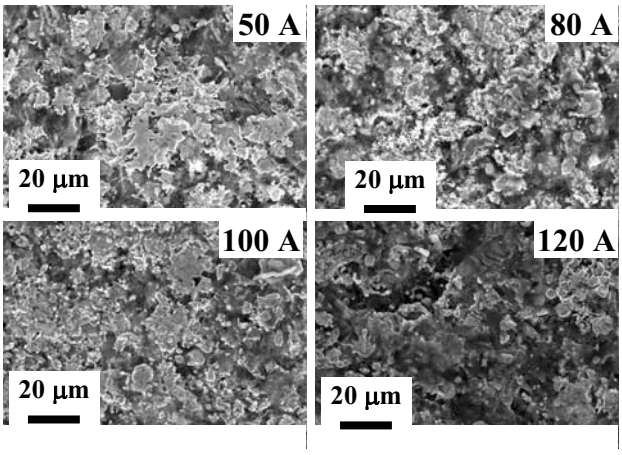

Fig. 5 Morphology of the sprayed W / SiC composites at various gun currents of 50, 80, 100 and 120 A.

In contrast, Baud et al. [16] reported the interfacial reactions between a W thin film and a single crystal (001) β-SiC substrate. They found the product phases W_5Si_3 and W_2C after annealing at 950 and 1100 °C.

Figure 4 shows SEM micrographs of the cross section of the plasma-sprayed W/SiC composite at various gun currents of 50,80, 100, and 120 A. The plasma-sprayed composite has two distinct regions. One region is a gray area occupied by SiC. The other one is a white area mostly corresponding to tungsten. The composite deposit was compact and we could not detect pores in the micrographs. One possible reason for the absence of pores in our deposit was the small mismatch in coefficient of the thermal expansion (CTE) of W and SiC, which is 4.02 x 10^{-6} and 4.5 x 10^{-6} /K, respectively. Another reason was the small thickness of the sprayed composite that ranged from 7 to 20 μm.

The morphology of the plasma-sprayed W/SiC composite surface at various gun current is depicted in **Figure 5**. Obviously, the white area corresponding to W decreased as a function of gun current. This data was in good agreement with XRD results (Fig. 3).

Some possible reactions from the mixture of W-SiC at high temperature can be written as follows:

$$SiC_{(s)} + CO_{2(g)} = Si_{(s)} + 2CO_{(g)} \quad (12)$$

$$SiC_{(s)} + CO_{2(g)} = Si_{(l)} + 2CO_{(g)} \quad (13)$$

$$SiC_{(s)} + 2CO_{(g)} = SiO_{2(s)} + 3C_{(s)} \quad (14)$$

$$CO_{(g)} + 1/2O_{2(g)} = CO_{2(g)} \quad (15)$$

$$SiC_{(s)} = Si_{(s)} + C_{(s)} \quad (16)$$

$$C_{(s)} + 1/2O_{2(g)} = CO_{(g)} \quad (17)$$

$$C_{(s)} + O_{2(g)} = CO_{2(g)} \quad (18)$$

$$SiC_{(s)} + O_{2(g)} = SiO_{2(s)} + C_{(s)} \quad (19)$$

$$SiC_{(s)} + O_{2(g)} = SiO_{(g)} + CO_{(g)} \quad (20)$$

$$SiC_{(s)} + 3/2O_{2(g)} = SiO_{2(s)} + CO_{(g)} \quad (21)$$

$$Si_{(s)} + 2CO_{2(g)} = SiO_{2(s)} + 2CO_{(g)} \quad (22)$$

$$Si_{(l)} + 2CO_{2(g)} = SiO_{2(s)} + 2CO_{(g)} \quad (23)$$

$$SiO_{2(s)} + CO_{(g)} = SiO_{(g)} + CO_{2(g)} \quad (24)$$

$$C_{(s)} + CO_{2(g)} = 2CO_{(g)} \quad (25)$$

As shown in fig.1, the mixture of W-SiC was introduced into the plasma jet, which is sealed from air, by the plasma gas and carrier gas, argon. Moreover, the plasma spray uses high temperatures (5000-12000 °C) and high velocities of (200-500 m/s). Therefore, the first decomposition of SiC in the argon atmosphere can be expressed as equation (16). It seems that the decomposition does not take place as expressed in

reactions (19) – (21) because there are silicon peaks instead of silicon oxide peaks in XRD, as seen in Fig. 3. But this is not evidence for the absence of silica in our composite because SiO_x is amorphous and difficult to detect especially if amounts are small.

3.3. Mechanical properties

Figure 6 shows the microhardness trend of plasma-sprayed W/SiC composites at various gun currents of 50, 80,100 and 120 A. Clearly, the hardness of the W /SiC composite deposit increased with decreasing input gun current. We believe the reason is that plasma-sprayed W /SiC composite deposited at a low gun current of 50 A was composed of monolithic SiC, W, and a very small amount of WO_3, while the composite sprayed at higher gun current contained a large amount of WO_3 and a small amount of Si. The hardness values exceeded those for pure annealed W (350-360 *Hv* [17, 18])) and are lower than those for SiC (2193 *Hv).* The addition of W particles to SiC decreased its hardness, one possible reason, due to the formation of softer, non equilibrium phases. The hardness trend was in good agreement with XRD data, which revealed the formation of tungsten oxides and free silicon at higher gun current.

The abrasive wear rate behavior of plasma-sprayed W/SiC composite is shown in **Figure 7**. Obviously, the abrasive wear rate decreases as a function of gun current. The composite produced at low gun current had the highest wear rate. It is known that one of the most important parameters controlling the wear behavior of a material is its hardness. The higher the hardness, the higher will be the abrasion resistance of the material. However, it has been found that other parameters such as hardening coefficient, compressive strength, toughness and ductility play an important role on the abrasion behavior of the metal matrix composite [19, 20)].

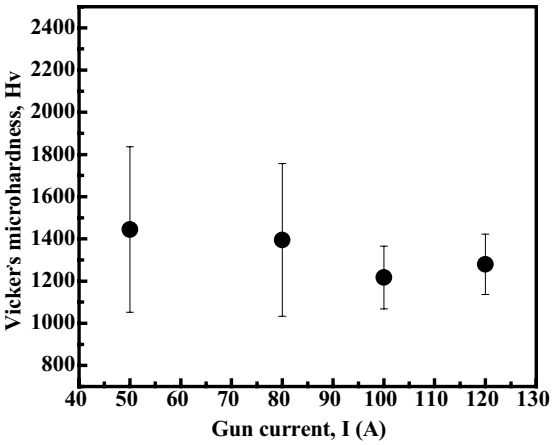

Fig. 6 Hardness of plasma-sprayed W/ SiC composite as a function of gun current.

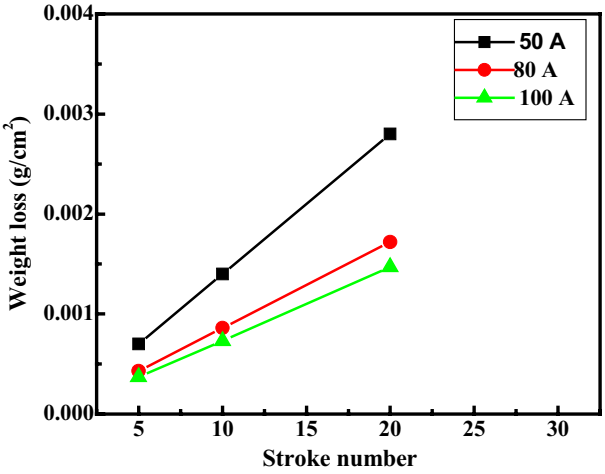

Fig. 7. Abrasive wear rate of plasma-sprayed W/SiC composite versus gun current.

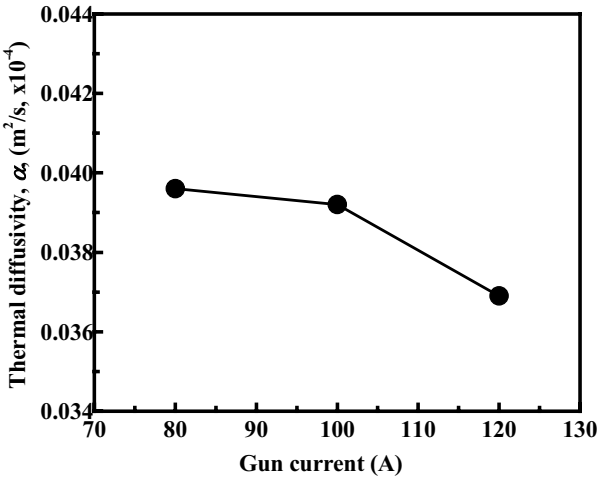

Fig. 8 Thermal diffusivity of plasma-sprayed W/ SiC composite versus input gun current.

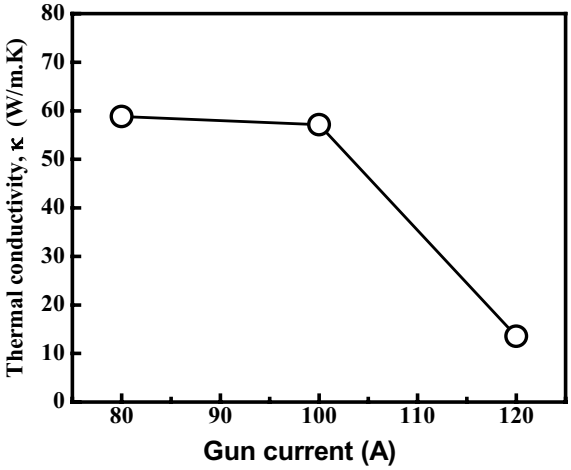

Fig. 9 Thermal conductivity of plasma-sprayed W/SiC composite versus input gun current.

3.4. Thermal diffusivity/conductivity properties

Figure 8 shows the thermal diffusivity of plasma-sprayed W /SiC composite versus the input gun current. Obviously, the thermal diffusivity of the W/SiC deposit decreased from (3.96×10^{-6} m^2/s) to (3.69×10^{-6} m^2/s) for deposits sprayed at 80, 120 A, respectively. This indicated that the tungsten oxidation and decomposition of SiC in the sprayed composite have a significant effect on the thermal diffusivity.

The thermal conductivity (TC) of plasma-sprayed tungsten/silicon carbide composite as a function of gun current is depicted in **Figure 9**. The thermal conductivity, *k*, decreased (from ~ 59 to 13.6 *W /m.K)* as the gun current increased from 80 to 120 A. These values were near to that reported for SiC/SiC composite fabricated by using CVR techniques (~ 75 W/m.K at 20 ^oC) [21]. Also, Gui et al. [22] studied the thermal conductivity of Al/SiC composite as a function of SiC particle size and its volume fraction. They found that the sprayed composites exhibit significantly lower thermal conductivity (from 87 to 38 W/m.K) than Al/SiC composites fabricated by other processes. They attributed the lower value of TC of the sprayed composites due to the interface between two sprayed layers, which act as a thermal barrier, and the thermal boundary resistance. Also, they suggested the hot rolling process to improve the TC of the composites.

4. Conclusions

W-SiC metal matrix composites have been prepared by atmospheric Gas tunnel type plasma spraying using a mixture of (12 % W - 88 wt. % SiC) as a feedstock powder. The effect of plasma gun current on the microstructure, mechanical and thermal properties of the sprayed composite was investigated. The principal conclusions from this study are as follows:

(1) Microstructure investigations revealed that the most of the W and SiC particles were melted and deposited on the AISI 304 substrate. The oxidation of W and decomposition of SiC increased as a function of input gun current.

(2) The hardness of the sprayed composite (~ 1450 *Hv)* was lower than that of pure monolithic SiC, which was attributed to the formation of WO_3 and the presence of dissociated Si phases in the structure of the composite.

(3) W/ SiC plasma sprayed composite had a low thermal conductivity of 59 W/mK at room temperature. The interface between two sprayed layers (thermal barrier) and the presence of impurities (like WO_3 and dissociated Si) are the dominant factors for low thermal conductivity in the sprayed composites.

References

1) V. Barabash, G. Federici, M. Rödig, L.Snead, C. H. Wu, J. Nucl. Mater. **283-287** (2000) 138.
2) S. Sampath, H. Herman, JOM **45** (7) (1993) 42.
3) Y. Arata, A. Kobayashi, Y. Habara, J. Appl. Phys. **62** (1987) 4884.
4) A. Kobayashi, Surf. Coat. Technol. **90** (1990) 197.
5) A. Kobayashi, S. Sharaft, N. Ghoniem, Surf. Coat. Technol. **200** (2006) 4630.
6) J. Gonzalez, P. Proulx, M. Boulos, J. Appl. Phys. **74** (1993) 3065.
7) É. Hegetüs, J. Neugebauer, M. Měszǎros, Int. J. Refract. Met. Hard Mater. **16** (1998) 67.
8) C. Bigey, L. Hilaire, G. Maire, J Catalysis **184** (1999) 406.
9) H-K Kang, SB Kang, Surf Coat Technol **182** (2004) 124.
10) N. El- Kaddah, J. Mckelliget, J. Szekely, Metall. Trans. B **15** (1984) 59.
11) S. Paik, X.Chen, P. Kong, E. Pfender, Plasma Chem. Plasma Process. **11** (1991) 229.
12) R. Smith, R. Knight, J. Met. **47** (1995) 32.
13) E. Pfender, Y.C. Lee, Plasma Chem. Plasma Process. **5** (1985) 211.
14) P.C. Huang, J. Heberlein, E. Pfender, Surf. Coat. Technol. **73** (1995) 142.
15) W. F. 1, P. A. Barnes, Mater. Sci. & Eng. B **72** (2000) 13.
16) L. Baud, C. Jaussaud, R. Madar, C. Bernard, JS Chen, MA Nicolet, Mater Sci Eng B **29** (1995) 126.
17) C.J. Smithells (Ed.), Smithells Metals Reference Book, seventh ed., Butterworth-Heinemann, Boston, 1992.
18) P. B. Bardes (Ed.), Metals Handbook, Vol. 2, ninth ed., American Society for Metals, Metals Park, 1979.
19) Z. Fang. Wear resistance of powder metallurgy alloys-powder metal technologies and applications, ASM Handbook.
20) J.A. Hawk, D.E. Alman, Mater. Sci. Eng A **239-240** (1997) 899.
21) W. Kowbel, K.T. Tsou, J.C. Withers, G.E. Youngblood,High thermal conductivity SiC:SiC composites for fusion applications-II, in Fusion Materials Semiann. Prog Rep. for period ending Dec. 31 1997, DOE:ER-0313:23, Oak Ridge National Lab, 1997, pp. 172–174.
22) M. Gui, S. B. Kang, K. Euh, Scripta Materialia **52** (2005) 51.